Preliminary communication/Communication

Synthesis and characterization of new pyrochlore solid solution $Bi_{1.5}Sb_{1.5-x}Nb_xCuO_7$

Mayouf Sellami [a],[*], Vincent Caignaert [b], Fatima Z. Kouadri Hanni [a], Noureddine Bettahar [a], Naceur Benhadria [a], Esmahan Sari-Mohammed [a], Safia Imine [a], Abdellah Bahmani [a]

[a] Laboratoire de chimie des matériaux inorganiques et applications (LCMIA), Faculté de chimie, Université des sciences et de la technologie d'Oran, BP 1505, 31000 El-Mnaouer Oran, Algeria
[b] Laboratoire de cristallographie et sciences des matériaux, ENSICAEN–CNRS UMR 6508, 6, boulevard du Maréchal-Juin, 14050 Caen cedex 4, France

A B S T R A C T

New pyrochlore solid solutions $Bi_{1.5}Sb_{1.5-x}Nb_xCuO_7$ have been synthesized ($0 \leq x \leq 1.5$) via the ceramic method in the air at 1000 °C. Rietveld refinement of the compounds $Bi_{1.5}Sb_{1.5-x}Nb_xCuO_7$ for $x = 0$, $x = 0.75$ and $x = 1.5$ by means of X-ray powder diffraction analysis confirmed an overall $A_2B_2O_7$ cubic pyrochlore structure according to $(Bi^{3+}_{1.5}Cu^{2+}_{0.5})(Sb^{5+}_{1.5-x}Nb^{5+}_xCu^{2+}_{0.5})O_7$ formula with 10.42009 (3) Å, 10.47193 (3) Å and 10.52679(4) Å, respectively, and $Fd\bar{3}m$ space group. Composition dependencies of cell parameters show a linear increase with the niobium x fraction. The magnetic susceptibility measurements achieved between 4 and 400 K indicate a paramagnetic behavior with an oxidation state "+2" for the copper ion. The electric resistivity measured using complex impedance spectroscopy evidences an increase of the electric conductivity with temperature and niobium substitution.

© 2013 Académie des sciences. Published by Elsevier Masson SAS. All rights reserved.

1. Introduction

Pyrochlore-type oxides have attracted great attention for a long time due to their remarkable physical and chemical properties as high thermal stability, high resistance to radiation damage and low thermal conductivity. These properties entitle them to extensive applications, for instance as catalysts [1,2], ionic/electric conductors [3], lithium ion batteries [4], radiation-damage-resistant materials [5], nuclear waste disposal [6,7], thermal barrier coatings [8] or solid electrolytes in high temperature fuel cells [9]. Pyrochlore oxides have the general formula $A_2B_2O_6O'$ with $z = 8$; A, B are cations and O, O' are anions. Most pyrochlore oxides crystallize in space group $Fd\bar{3}m$ (#227). Of the four possible choices of origin in this space group, the most commonly used places are the smaller B-type cation at the 16c site with the larger A-type cation at 16d. There are two anion sites, with O at 48f, and O' at 8b. There are only two variable structural parameters, the cubic lattice parameter a, and the positional parameter x, for the O atom in 48f. The pyrochlore structure can be described as interpenetrating BO_6 octahedra and A_2O' chains [10,11]. The B_2O_6 framework consists of $[BO_6]$ octahedra sharing all vertices to form large cavities [12]. From extensive experimental work on the synthesis and structural characterization of cubic pyrochlores, stability fields have been proposed for allowable substitution into the A and B cation sites based on measures, such as the ratio of the cation radii size and the cation electronegativity [13]. These new pyrochlore solid solutions $Bi_{1.5}Sb_{1.5-x}Nb_xCuO_7$ will be used in the future as catalysts [14]. Here, we report the synthesis and

* Corresponding author.
E-mail address: mourad7dz@yahoo.fr (M. Sellami).

the study of the corresponding structural, magnetic and electric properties.

2. Experimental

The solid solutions were prepared by solid-state reaction of stoichiometric amounts of reagent-grade Bi_2O_3 (99.9%), Sb_2O_3 (99%), Nb_2O_5 (99%) and CuO (99%) (Aldrich Chemical Company Ltd). The mixtures were ground for 1 h with an agate mortar and pestle. The resulting powders were calcined at 500 °C for 24 h in an alumina crucible. Then, the powders were again ground and calcined two more times successively at 700 °C and 900 °C for 48 h each. The resulting powders were re-milled for 1/2 h and uniaxially pressed into pellets about 13 mm in diameter and 2 mm in thickness. Then, they were sintered at 1000 °C for 48 h in the air. The samples' color was brown. The specimens were initially characterized by X-ray powder diffraction using a PANalytical X'Pert Pro X-ray diffraction system. Data were collected using Cu Kα radiation. Rietveld refinement [15] of the X-ray powder diffraction data was carried out using the FULLPROF program [16]. Polished specimens were examined using a conventional Philips SEM XL30 scanning electron microscope. The magnetic susceptibility of powder samples was measured from 4 to 400 K with SQUID. Electrical conductivity measurements were carried out using an impedance lock-in EG&G 7220-type with a 10-mV AC signal amplitude at frequencies between 30 Hz and 120 kHz.

3. Results and discussion

3.1. Structural characterization

3.1.1. Study of $Bi_{1.5}Sb_{1.5-x}Nb_xCuO_7$ solid solution

Previous studies [17] showed that the substitution of copper by manganese in compound $Bi_{1.5}Sb_{1.5}CuO_7$ [18] forms a continuous solid solution with a pyrochlore structure. Here, we substitute antimony by niobium according to this system: $Bi_{1.5}Sb_{1.5-x}Nb_xCuO_7$. Fig. 1 shows X-ray diffraction patterns of as-synthesized $Bi_{1.5}Sb_{1.5-x}Nb_xCuO_7$. All the diffraction lines in each pattern can be well indexed in the pyrochlore pattern

(ICSD 01-077-8429). The results indicated that all compounds had a single cubic pyrochlore structure of $Bi_{1.5}Sb_{1.5-x}Nb_xCuO_7$ belonging to space group $Fd\bar{3}m$ (No. 227). Using Scherrer's equation [19], the crystallite sizes of the samples were calculated from the size effect contribution to the peak half-width of the (2 2 2) peak and were found to be in the 100–140 nm range. These size limits depend on the ceramic preparation method (high temperature). It was worth noting that the diffraction peaks of the samples were shifted toward a smaller diffraction angle as a result of the increasing Nb doping content, indicating that the lattice parameters had increased according to Vegard's law [20] Effectively, the cell parameters were practically on the correlation line, indicating that the difference between the niobium ionic radius, $R_{Nb}(VI) = 0.72$ Å, and the antimony ionic radius, $R_{Sb}(VI) = 0.60$ Å [21], is the reason of this increase in the lattice constant. Fig. 2 shows SEM photographs of the surface morphologies of the disk samples. It was found that the grain size of the samples slightly changes with increasing x. Samples with $x = 0$ and 0.5 seem to be rounded, whereas sharp grain edges are evidenced for $x = 1$. The difference in the grain growth rate during sintering, which causes the variation in grain size, is attributed to the different diffusion rates of the ionic species.

3.1.2. Structural refinement

The highly symmetrical ideal pyrochlore structure $A_2B_2O_7$ crystallizes in space group $Fd\bar{3}m$ with A and B cations on two special positions (16d, 16c) and oxygen atoms on two sites, 48f O and 8b O′, resulting in a single positional variable (x for the 48f site oxygen atoms in the B_2O_6 octahedral network). Rietveld refinement with this model shows that copper is statistically distributed on the A and B sites, leading to formula $(Bi_{1.5}Cu_{0.5})(Sb_{1.5-x}Nb_xCu_{0.5})O_7$. As expected, this model results in anomalously large thermal parameters for the A site cations and the O′ oxygen atoms in this initial refinement. The disordered structure was therefore modelled assuming static displacements of the A and O′ atoms, similar to that of analogous Bi–M–Nb–O pyrochlores (M = Zn [22], Fe [23], Mn [24]), whose structures were refined using neutron powder diffraction data. The refinement of the
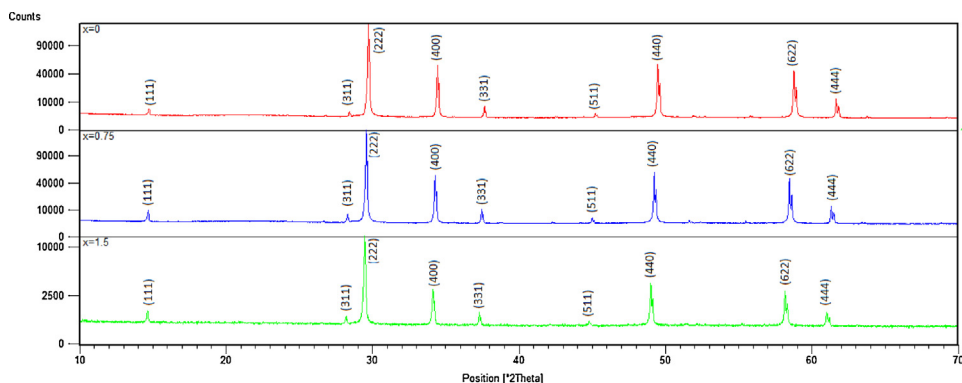

Fig. 1. (Color online.) XRD patterns of $Bi_{1.5}Sb_{1.5-x}Nb_xCuO_7$ solid solutions.

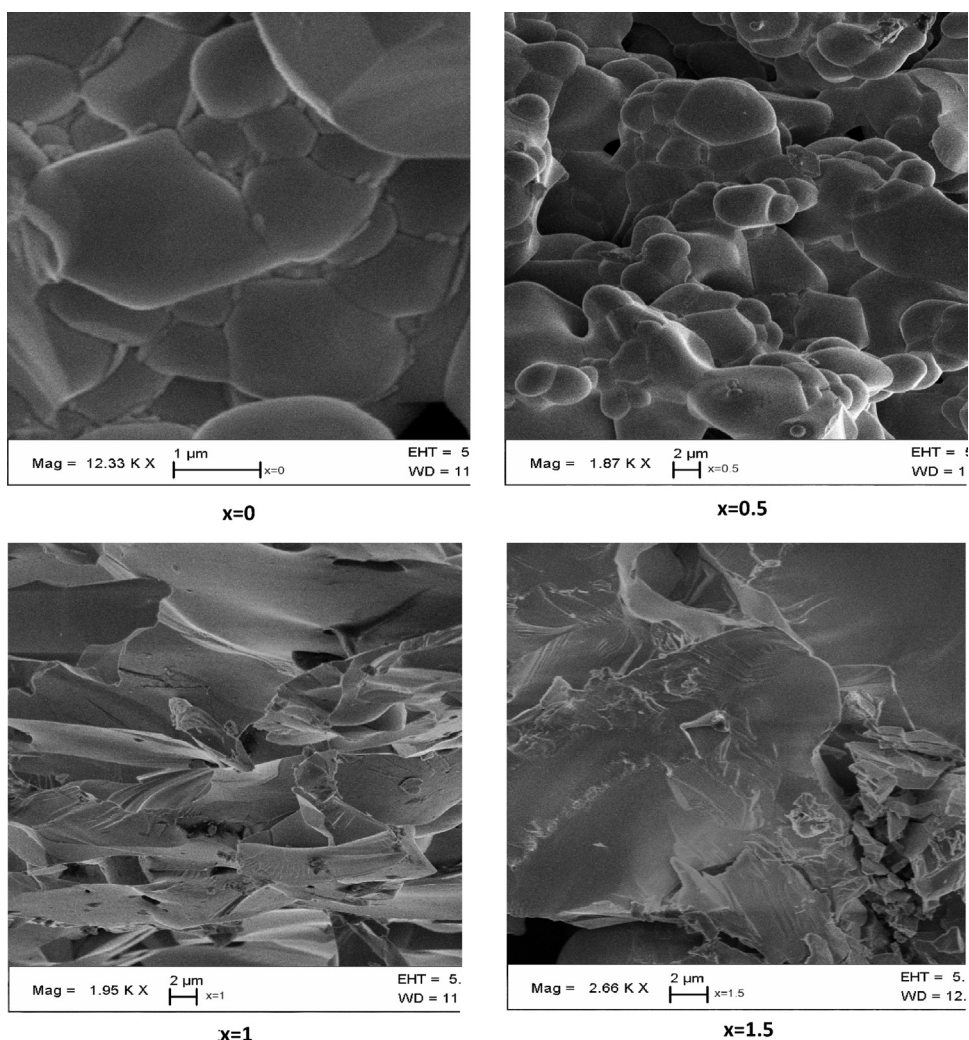**Fig. 2.** SEM micrograph of $Bi_{1.5}Sb_{1.5-x}Nb_xCuO_7$ compounds ($x = 0$; $x = 0.5$; $x = 1$; $x = 1.5$).

positional parameters for the disordered metal sites was carried out assuming displacements of the A_2O' network, as found for a number of other pyrochlore compounds [25–28]. Refinement without displacement of the A site Bi/Cu gave bad residuals for the smallest reflections. Improved results were obtained with Bi/Cu displaced to six partially filled 96g sites and O′ site displaced to the 32e site. Observed, calculated and difference X-ray powder diffraction spectra are displayed in Fig. 3. The agreement between the observed and calculated profile is excellent and R_{Bragg} factors ≤ 6.54; they depend on both the atomic coordinates and the chemical composition. The final refinement results are given in Tables 1 and 2. The pyrochlore structure, $(Bi_{1.5}Cu_{0.5})(Sb_{1.5-x}Nb_xCu_{0.5})O_7$, can be described by the interpenetrating networks of $(Sb_{1.5-x}Nb_xCu_{0.5})O$ octahedra and intersecting $(Bi_{1.5}Cu_{0.5})O'$ chains, where A cations are in the 96g position and O′ anions are in the 32e position. Fig. 4 illustrates the displacive disorder of the A_2O' network. The arrangement of the octahedra, sharing vertices, generates hexagonal cavities where the A sites are located. The little red spheres

represent the oxygen atoms and the yellow spheres are niobium/copper atoms. The blue spheres represent the six equivalent 96g sites for the A site Bi/Cu cations, and the large red spheres denote the 4 possible displaced positions
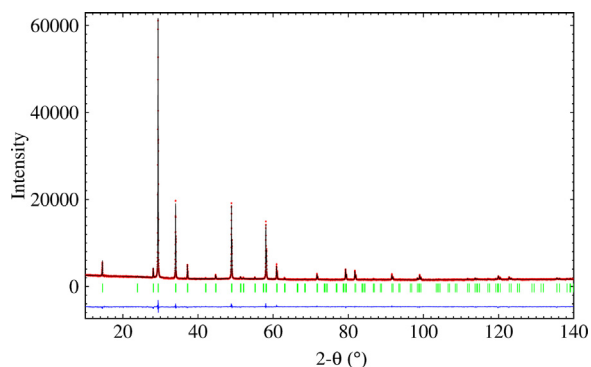

Fig. 3. (Color online.) Observed, calculated and difference X-ray powder diffraction patterns of $Bi_{1.5}Nb_{1.5}CuO_7$.

Table 1
Rietveld refinement results of $Bi_{1.5}Sb_{1.5-x}Nb_xCuO_7$ solid solutions.

Sample	$x = 0$	$x = 0.75$	$x = 1.5$
Global formula	$Bi_{12}Cu_8Sb_{12}O_{56}$	$Bi_{12}Cu_8Sb_6Nb_6O_{56}$	$Bi_{12}Cu_8Nb_{12}O_{56}$
Formula mass	5373.6 g	5200.2 g	5026.88 g
Crystalline system	Cubic	Cubic	Cubic
Space group	$Fd\bar{3}m$	$Fd\bar{3}m$	$Fd\bar{3}m$
Cell parameter	10.42009(3) Å	10.47193(3) Å	10.52679(4) Å
Cell volume	1131.393(6) Å^3	1148.366(6) Å^3	1166.510(8) Å^3
Wyckoff sequence	$fdcb$	$fdcb$	$fdcb$
Number of reflexion	74	74	73
Number of refined parameters	14	17	14
Function profile	Pseudo-Voigt	Pseudo-Voigt	Pseudo-Voigt
R_{wp}	3.67	3.35	2.97
R_p	2.59	2.41	2.36
R_{exp}	2.03	1.86	2.32
R_{Bragg}	6.51	5.72	6.54

Table 2
Atomic positions and site occupancies from Rietveld refinement results of $Bi_{1.5}Sb_{1.5-x}Nb_xCuO_7$ solid solutions.

	Atom	Position	Site occupancy	x	y	z	B_{iso} [Å^2]
$x = 0$	Bi(1)/Cu(1)	96g	0.125/0.041	0.5076(7)	0.5076(7)	0.4709(9)	0.10(9)
	Sb(2)/Cu(2)	16c	0.75/0.25	0	0	0	0.10(5)
	O1	48f	1	0.3243(9)	1/8	1/8	1.7(3)
	O2	32e	1/4	0.346(3)	0.346(3)	0.346(3)	1.7(3)
$x = 0.75$	Bi(1)/Cu(1)	96g	0.125/0.041	0.5101(7)	0.5101(7)	0.4705(9)	0.10(9)
	Sb(2)/Nb(2)/Cu(2)	16c	0.375/0.375/0.25	0	0	0	0.60(9)
	O1	48f	1	0.3239(8)	1/8	1/8	1.4(3)
	O2	32e	1/4	0.342(1)	0.342(1)	0.342(1)	1.4(3)
$x = 1.5$	Bi(1)/Cu(1)	96g	0.125/0.041	0.5140(9)	0.5140(9)	0.4697(9)	0.90(9)
	Nb(2)/Cu(2)	16c	0.75/0.25	0	0	0	0.10(4)
	O1	48f	1	0.3154(6)	1/8	1/8	1.4(3)
	O2	32e	1/4	0.354(3)	0.354(3)	0.354(3)	1.4(3)
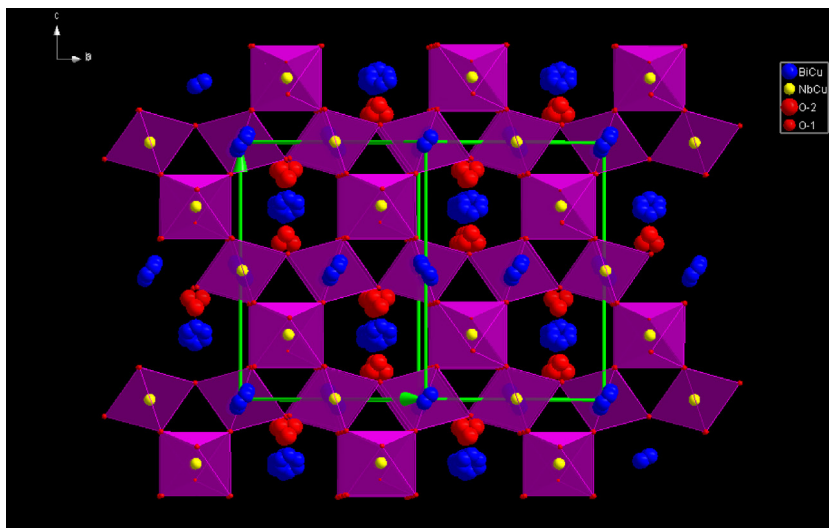
Fig. 4. (Color online.) $(Bi_{1.5}Cu_{0.5})(Nb_{1.5}Cu_{0.5})O_7$ cubic pyrochlore structure.

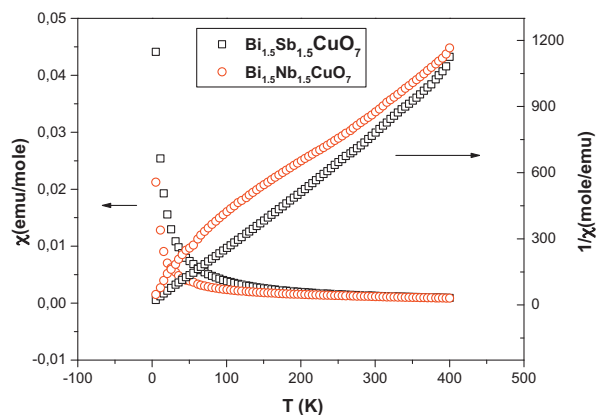**Fig. 5.** (Color online.) Susceptibility and inverse susceptibility versus temperature of $Bi_{1.5}Sb_{1.5}CuO_7$ and $Bi_{1.5}Nb_{1.5}CuO_7$.

for the O′ oxygens. (For interpretation of the references to color in Fig. 4, the reader is referred to the web version of this article).

3.2. Magnetic susceptibility

Magnetic data obtained for the compounds indicate that the samples were overall paramagnetic in nature, with an effective moment of 1.74(5) and 1.70(3) μ_B for the copper in compounds $Bi_{1.5}Sb_{1.5}CuO_7$ and $Bi_{1.5}Nb_{1.5}CuO_7$. The inverse susceptibility versus temperature data for the $Bi_{1.5}Nb_{1.5}CuO_7$ show upward curvature at the lowest temperatures and at high temperatures deviate somewhat from a linear Curie–Weiss behavior (regions between 200 and 300 K). The observed effective magnetic moments (μ_{eff}/mol Cu), calculated from the slopes of the Curie–Weiss fits indicates the "2 +" oxidation state of the copper. The temperature dependence of the magnetic susceptibility and its inverse are shown in Fig. 5. The copper oxidation state confirm the pyrochlore formula (1.5–1.5–1-7 compound), since bismuth has a "3 +" and niobium and antimony [29] have a "5 +" oxidation state.
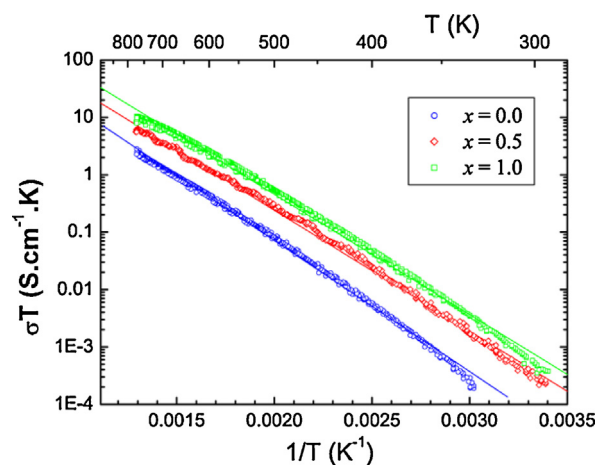
3.3. Electrical characterization

Fig. 6 shows the temperature dependence of the total conductivity of $Bi_{1.5}Sb_{1.5-x}Nb_xCuO_7$ ceramics, obtained from AC electrical measurements and impedance plots over the temperature range between 300 and 800 K in the air. Clearly, the total conductivity of $Bi_{1.5}Sb_{1.5-x}Nb_xCuO_7$ ceramics gradually increases with increasing temperature from 300 to 800 K. The temperature dependence of the total conductivity of $Bi_{1.5}Sb_{1.5-x}Nb_xCuO_7$ ceramics can be described by the Arrhenius equation, $\sigma T = \sigma_0 \exp(-E/k_B T)$ where σ, T, σ_0, E, and k_B are the total conductivity, absolute temperature, pre-exponential factor, activation energy and Boltzmann constant, respectively. The total conductivity data follow a linear behavior, which confirms that the electrical conductivity process is thermally activated. The activation energy for the total conductivity of $Bi_{1.5}Sb_{1.5-x}Nb_xCuO_7$ ceramics slightly decrease with increasing the niobium content. The activation energies were determined as 0.45, 0.42 and 0.41 eV for the samples doped with $x = 0$, 0.5 and 1, respectively. The decrease in the activation energy is the result of an increasing in the conductivity with increasing the Nb content, and reflects the impurity level shift toward the conduction or valence band by increasing the number of sharing electrons or holes. All compounds are considered as semi-conductors.

4. Conclusion

A new pyrochlore solid solution with formula $Bi_{1.5}Sb_{1.5-x}Nb_xCuO_7$ was synthesized by solid-state reaction at 1000 °C. All samples had a single cubic pyrochlore structure of $Bi_{1.5}Sb_{1.5-x}Nb_xCuO_7$ with space group $Fd\bar{3}m$ (No. 227). The lattice constant increased linearly with increasing niobium concentration. Rietveld refinements confirmed an overall $B_2O_6 \cdot A_2O'$ cubic pyrochlore structure with Cu cations on both A and B sites. Magnetic characterization measurements confirmed a "+2" oxidation state of the copper cation. Electric measurements at high temperature revealed an increase in the electrical conductivity, with a decrease in the activation energy. Our synthesized compounds are considered as semi-conductors.

Fig. 6. (Color online.) Conductivity variation versus inverse temperature (1/T) of $Bi_{1.5}Sb_{1.5-x}Nb_xCuO_7$ compound.

References

[1] J.M. Sohn, M.R. Kim, S.I. Woo, Catal. Today 83 (2003) 289.
[2] K. Li, H. Wang, H. Yan, J. Mol. Catal. A: Chem. 249 (2006) 65.
[3] T. Yu, H.L. Tuller, Solid State Ionics 177 (1996) 86.
[4] N. Sharma, G.V. Rao Subba, B.V.R. Chowdari, J. Power Sources 159 (2006) 340.
[5] K.E. Sickafus, L. Minervini, R.W. Grimes, J.A. Valdez, M. Ishimaru, F. Li, K.J. McClellan, T. Hartmann, Science 289 (2000) 748.
[6] J. Lian, S.V. Yudintsev, S.V. Stefanovsky, L.M. Wang, R.C. Ewing, J. Alloys Compd. 444–445 (2007) 429.

[7] S. Lutique, D. Staicu, R.J.M. Konings, V.V. Rondinella, J. Somers, T. Wiss, J. Nucl. Mater. 319 (2003) 59.

[8] X.Q. Cao, J. Mater. Sci. Technol. 23 (2007) 15.

[9] J. Garcia-Barriocanal, A. Rivera-Calzada, M. Varela, Z. Sefrioui, M.R. Díaz-Guillén, K.J. Moreno, J.A. Díaz-Guillén, E. Iborra, A.F. Fuentes, S.J. Pennycook, C. Leon, J. Santamaría, Chem. Phys. Chem. 10 (2009) 1003.

[10] M.A. Subramanian, G. Aravamudan, G.V.S. Rao, Prog. Solid State Chem. 15 (1983) 55.

[11] B.C. Chakoumakos, J. Solid State Chem. 53 (1984) 120.

[12] H. Von Gaertner, Neues Jahrb. Miner. Geol. Palaeontol. 61 (1931) 1.

[13] J.C. Nino, Materials Science and Engineering, The Pennsylvania State University, University Park, PA, 2002.

[14] M. Sellami, F. Merabat, N. Bettahar, A. Bahmani, S. Imine, E. Sari-mohamed, N. Benhadria, Synthèse et caractérisation d'une nouvelle solution solide de type pyrochlore de formule $Bi_{1.56}Sb_{1.48}Co_{0.96-x}Fe_xO_7$, in: VIIIes Journées internationales de chimie, Université Mentouri, Constantine, Algeria, 12–13 December, 2012.

[15] M.A. Subramanian, B.H. Toby, A.P. Ramirez, W.J. Marshall, A.W. Sleight, G.H. Kwei, Science 273 (1996) 81.

[16] C.A. Mims, A.J. Jacobson, R.B. Hall, J.T. Lewandowski, J. Catal. 153 (2) (1995) 197.

[17] M. Sellami, V. Caignaert, M. Hamdad, A. Bekka, N. Bettahar, J. Alloys Compd. 482 (2009) 13.

[18] M. Sellami, A. Bekka, N. Bettahar, C. R. Chimie 8 (2005) 1129.

[19] A.L. Patterson, The Scherrer formula for X-ray particle size determination, Phys. Rev. 56 (1939) 978.

[20] A.R. West, Solid State Chemistry and its Applications, Wiley, New Delhi, 1984.

[21] R.D. Shannon, Acta Crystallogr. A32 (1976) 751.

[22] I. Levin, T.G. Amos, J.C. Nino, T.A. Vanderah, C.A. Randall, M.T. Lanagan, J. Solid State Chem. 168 (2002) 69.

[23] M.W. Lufaso, T.A. Vanderah, I.M. Pazos, I. Levin, J.C. Nino, V. Provenzano, P.K. Schenck, J. Solid State Chem. 179 (2006) 3900.

[24] T.A. Vanderah, M.W. Lufaso, A.U. Adler, I. Levin, J.C. Nino, V. Provenzano, P.K. Schenck, J. Solid State Chem. 179 (2006) 3467.

[25] M. Ganne, K. Toyama, Mater. Res. Bull. 10 (1975) 1313.

[26] M. Avdeev, M.K. Haas, J.D. Jorgensen, R.J. Cava, J. Solid State Chem. 24 (2002) 169.

[27] L.Q. Li, B.J. Kennedy, Chem. Mater. 15 (2003) 4060.

[28] U. Ismunandar, T. Kamiyama, K. Oikawa, A. Hoshikawa, B.J. Kennedy, Y. Kubota, K. Kato, Mater. Res. Bull. 39 (2004) 553.

[29] M. Sellami, N. Ngyen, A. Bekka, N. Bettahar, C. R. Chimie 9 (2006) 1209.